Cell

Mechanism of Transcription Initiation at an Activator-Dependent Promoter Defined by Single-Molecule Observation

Larry J. Friedman[1,*] and Jeff Gelles[1,*]
[1]Department of Biochemistry, Brandeis University, Waltham, MA 02454-9110, USA
*Correspondence: larryfj@brandeis.edu (L.J.F.), gelles@brandeis.edu (J.G.)
DOI 10.1016/j.cell.2012.01.018

SUMMARY

Understanding the pathway and kinetic mechanisms of transcription initiation is essential for quantitative understanding of gene regulation, but initiation is a multistep process, the features of which can be obscured in bulk analysis. We used a multiwavelength single-molecule fluorescence colocalization approach, CoSMoS, to define the initiation pathway at an activator-dependent bacterial σ^{54} promoter that recapitulates characteristic features of eukaryotic promoters activated by enhancer binding proteins. The experiments kinetically characterize all major steps of the initiation process, revealing heretofore unknown features, including reversible formation of two closed complexes with greatly differing stabilities, multiple attempts for each successful formation of an open complex, and efficient release of σ^{54} from the polymerase core at the start of transcript synthesis. Open complexes are committed to transcription, suggesting that regulation likely targets earlier steps in the mechanism. CoSMoS is a powerful, generally applicable method to elucidate the mechanisms of transcription and other multistep biochemical processes.

INTRODUCTION

DNA transcription by multisubunit RNA polymerases (RNAPs) is a central process through which gene expression is regulated in all organisms. In bacteria, transcription regulation is a key determinant of evolutionary fitness that enables a species to effectively compete for environmental resources (Cases et al., 2003). A quantitative understanding of the mechanisms of transcription regulation is required to (1) understand the dynamic response of gene transcription to environmental stimuli, (2) reliably define the systems behavior of regulatory networks, or (3) rationally design synthetic networks. This necessitates identifying reaction intermediates, defining the rates of individual reaction steps, and determining which steps are modulated by regulators. It is particularly important to address these questions for initiation, the most heavily regulated phase of transcription (Browning and Busby, 2004). Furthermore, transcription initiation is the target of antibacterial drugs in widespread clinical use (Darst, 2004; Ho et al., 2009). Clear understanding of the initiation pathway is therefore essential to understanding development of drug resistance and to rational design of combination therapies (Villain-Guillot et al., 2007).

Transcription promoter recognition in bacteria is mediated by σ initiation subunits. In complex with core RNAP, σ recognizes and directly binds to promoter-specific DNA sequences. After binding, the polymerase-DNA complex proceeds through a series of conformational intermediates before forming a mature transcription elongation complex capable of processive RNA synthesis.

For several bacterial promoters dependent on the major σ^{70} subunit, key steps in initiation have been identified using kinetic and intermediate trapping experiments (Saecker et al., 2011). Furthermore, footprinting and crystallographic analysis have revealed identities and structures of some intermediates in the initiation pathway (Davis et al., 2007; Murakami and Darst, 2003; Sclavi et al., 2005). After initiation, elongation complexes have been reported to release or retain σ^{70} to varying degrees (Bar-Nahum and Nudler, 2001; Deighan et al., 2011; Kapanidis et al., 2005).

Some bacterial promoters are dependent on the less studied σ^{54} subunit (Buck et al., 2000; Joly et al., 2012), the major alternative σ factor in many bacterial species. σ^{54} is nonhomologous with σ^{70} (Merrick, 1993), and σ^{54}RNAP has functional properties distinct from RNAPs containing other σ factors. Gene expression by σ^{54}RNAP requires activator ATPases, which bind to promoter-distal enhancer DNA sequences (Buck et al., 2000; Popham et al., 1989; Wigneshweraraj et al., 2008). Environmental cues turn on specific activators that, in turn, enhance transcription initiation at one or more σ^{54}-dependent promoters (Reitzer and Schneider, 2001).

Here, we studied the prototypical σ^{54} promoter of the *S. typhimurium glnALG* operon, at which initiation is activated by the NtrC activator protein in response to low environmental nitrogen (Magasanik, 1996). σ^{54}RNAP binds at this promoter to form transcriptionally silent (Ninfa et al., 1987; Sasse-Dwight and Gralla, 1988) closed complexes in which DNA remains base-paired (Popham et al., 1989). When ATP and NtrC (either the phosphorylated wild-type protein or a constitutively active mutant; Klose et al., 1993) are added, σ^{54}RNAP melts a short

DNA segment, forming long-lived open promoter complexes (Popham et al., 1989; Wedel and Kustu, 1995). Subsequent addition of nucleoside triphosphates (NTPs) enables the polymerase to begin transcript synthesis and depart the promoter. The NtrC/σ^{54} system is of particular interest because though biochemically more simple, it nonetheless recapitulates key functional properties of large classes of eukaryotic RNAP II promoters that are activated through transcriptional enhancers and enhancer binding proteins (Lin et al., 2005; Sasse-Dwight and Gralla, 1990). These properties include the formation of transcriptionally quiet unactivated RNAP-promoter complexes, the requirement for an ATPase to open the transcription bubble, conversion of inactive to active transcription factors by post-translational modification, and "action at a distance" activation of RNAP by a transcription factor that binds to an enhancer DNA sequence that functions independently of orientation and with only a weak dependence on position.

For all types of bacterial and eukaryotic transcription promoters, the large number of different states of the polymerase-promoter complex means that full experimental elucidation of the pathway of functional initiation is difficult. Because a mixture of different states is present in a molecular ensemble, evidence for reaction intermediates or alternative pathways (Susa et al., 2006) can be indirect or subtle (Kontur et al., 2008), and access to the rates connecting those intermediates is often limited (Haugen et al., 2006). The advent of single-molecule optical methods has raised the possibility of circumventing some of these problems by directly observing initiation at single promoters one molecule at a time (Revyakin et al., 2004, 2006).

Here, we present the application to transcription initiation of a single-molecule approach that reveals initiation intermediates in the context of the full initiation pathway and quantitatively defines initiation dynamics. Colocalization single-molecule spectroscopy (CoSMoS) visualizes spectrally distinguishable dye labels that are placed on different proteins and/or nucleic acids that participate in a biochemical pathway (Crawford et al., 2008; Friedman et al., 2006; Hoskins et al., 2011). Using CoSMoS, we directly visualize on single DNA molecules all major steps in initiation, including polymerase binding, open complex formation, transcript production, and σ^{54} departure. Quantitative analysis of these observations reveals the mechanism and full dynamics of initiation at an activator-dependent transcription promoter.

RESULTS

Visualizing the Initiation Reaction on Single DNA Molecules

To visualize open complex formation and subsequent transcript production at a σ^{54} promoter, we first immobilized a biotin-tagged template DNA containing the promoter (Figure 1A and Figure S1A available online) on the streptavidin-conjugated surface of a flow chamber (Figure 1B, left). Individual DNA molecules were detected through the fluorescence of an attached Alexa Fluor 488 (AF488) dye using a total internal reflection fluorescence (TIRF) microscope (Friedman et al., 2006). At this surface density of DNA, images show discrete, well-separated spots of AF488 fluorescence corresponding to individual DNA molecules (Figure 1C).

We next introduced into the flow chamber σ^{54}RNAP labeled on the σ^{54} subunit with Cy3 dye, ATP, and the constitutively active S160F, D54E mutant of NtrC (Klose et al., 1993; hereafter denoted simply NtrC) to form open complexes. In TIRF microscopy, fluorescence is excited only within ~100 nm of the surface. Diffusion of Cy3-σ^{54}RNAP molecules through this thin layer contributes only minimal, diffuse background fluorescence. In contrast, a fluorescent RNAP bound to a surface-attached DNA creates a tethered fluorescence source visualized as a well-defined spot. Such spots appeared and accumulated over ~40 min until most detected templates had a colocalized Cy3-σ^{54}RNAP spot. The spots remained even 15 min after flushing unbound Cy3-σ^{54}RNAP from the chamber (Figure 1D). Ninety percent of RNAP spots (43/48) had colocalized template molecules (Figure 1F). Few or no DNA molecules had colocalized polymerase spots in controls with promoter-deleted (<1%; 1/231) or enhancer-deleted (8%; 10/123) DNAs, compared with 74% (75/101) for DNA with the promoter. Thus, there is little nonspecific binding of polymerase to DNA or to the surface, and 90% of template molecules are labeled. Taken together, these results confirm that the Cy3 spots represent promoter-specific complexes of RNAP with DNA.

To verify that the DNA-colocalized RNAP spots are from transcriptionally competent open complexes, we introduced buffer containing ATP, CTP, and GTP (but no RNAP or NtrC) and a Cy5-labeled oligonucleotide probe that can hybridize to transcript. Because UTP is absent, open complexes should be converted into stalled elongation complexes each with a protruding nascent transcript (Figure 1B). We detected transcript production as an accumulation of long-lived fluorescence spots (Figure 1E) that resulted from hybridization of one or more transcript probes (Figures S1E and S1F).

Few probe spots were seen in control experiments in which NtrC or ATP was not present during the initial incubation, confirming that the spots report transcript production as opposed to nonspecific surface binding of probe or hybridization to the DNA template (Figures S1B–S1D). Nearly all (89%; 175 of 197) transcript spots coincided with the preformed open complexes (Figure 1G), confirming that RNAP was efficiently dye labeled and transcriptionally active. The majority (typically > 75%, e.g., 98 of 130) of Cy3 complex locations show the Cy5 transcript signal promptly (within 2 min) after addition of nucleotides. Thus, the experiment efficiently detected both promoter-binding and activator-dependent transcript formation by single dye-labeled RNAP molecules.

Rapid Formation of the Closed Promoter Complex

Initial binding of RNAP leading to the formation of a closed complex is a key step in promoter recognition. This process has previously been characterized for σ^{70}RNAP by indirect methods, primarily in experiments that measure only the equilibrium constant rather than the binding and dissociation kinetics (reviewed in Record et al., 1996; Saecker et al., 2011; see also Haugen et al., 2006). Here, the ability to detect single polymerase and template molecules allowed us to directly examine the binding kinetics. We examined Cy3-σ^{54}RNAP binding to Cy5 template in the absence of NtrC and nucleotides (Figure 2A), conditions in which the reaction does not proceed beyond

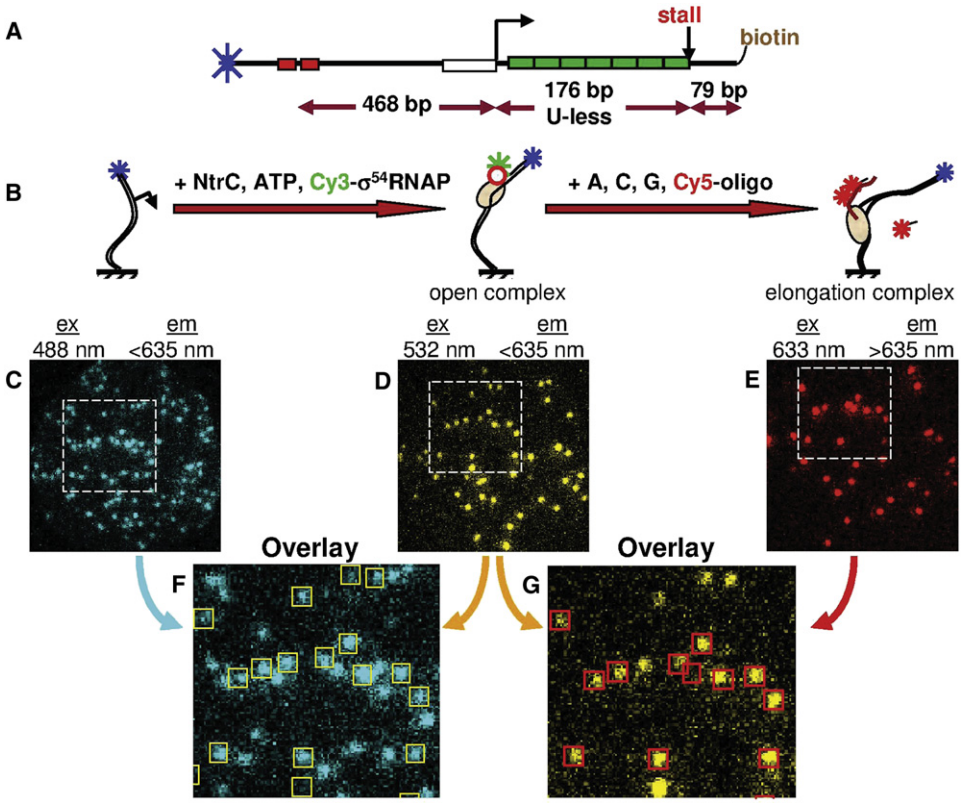

Figure 1. Single-Molecule Observation of Open Complex Formation and Transcript Production

(A) Template schematic. The template contains NtrC-binding enhancer site (red), the *glnAP2* σ^{54}RNAP-binding site (white box) and start site (bent arrow), and a transcribed region encoding a U-less RNA containing seven repeats of a 21 bp cassette (green).

(B) Stepwise single-molecule transcription experiment. Surface-tethered template molecules (left) form open complexes (middle) with holoenzyme comprised of Cy3 (green star)-σ^{54} (circle) and core RNAP (ellipse). After transcript production (right), the RNA is detected by hybridization of a Cy5 (red star)-labeled DNA complementary to the repeat cassette. In this and all other experiments in this paper, there is no FRET because the distances separating the dyes are too large.

(C–E) False color images (17.6 × 17.6 μm) of a surface region acquired at the three reaction stages depicted in (B). Fluorescence excitation (ex) and emission (em) wavelengths selectively image AF488 (C), Cy3 (D), or Cy5 (E).

(F) Positions of spots in the highlighted region of (D) (yellow squares) overlaid with the corresponding region of (C).

(G) Positions of spots in the highlighted region of (E) (red boxes) overlaid with the corresponding area of (D).

See also Figure S1.

closed complex formation (Popham et al., 1989). As before, polymerase colocalized with DNA (Figure 2B), but in the absence of activator RNAP, binding events were only transient (Figures 2C and 2D).

We measured the time elapsed up to when the first RNAP bound to each template molecule (Figure 2D, red). The resulting second-order rate constant for formation of the initial closed complex, 2.1×10^7 M^{-1} s^{-1} (Figure 2E), approaches but does not exceed the maximum possible through three-dimensional diffusion in solution (Halford, 2009). Addition of NtrC and ATP did not change the rate (Figure S2), suggesting that NtrC does not significantly assist kinetic recruitment of RNAP to the promoter.

σ^{54}RNAP Forms Two Kinds of Closed Complexes

Strikingly, σ^{54}RNAP closed complexes were kinetically unstable: at equilibrium, we saw multiple RNAP binding and dissociation events on each DNA molecule (Figures 3A and 3B). Furthermore, the distribution of complex lifetimes clearly showed two exponential components (Figures 3C and S3), revealing the presence of at least two distinct types of closed complexes. The results are consistent with a minimal sequential kinetic scheme:

$$R + P \underset{k_{-1}}{\overset{k_1}{\rightleftharpoons}} RP_1 \underset{k_{-2}}{\overset{k_2}{\rightleftharpoons}} RP_2, \quad (1)$$

in which RP_1 and RP_2 are different closed complexes. Quantitative analysis of the data in Figures 2 and 3 (see Extended Experimental Procedures) determined the four rate constants and thereby specified the essential features of closed complex formation based on this scheme: whereas a stable, long-lived closed complex (RP_2) is the predominant species at equilibrium (93% population), there is nevertheless a distinct, promoter-specific, short-lived closed complex (RP_1) that, in this model, is a required precursor to formation of RP_2.

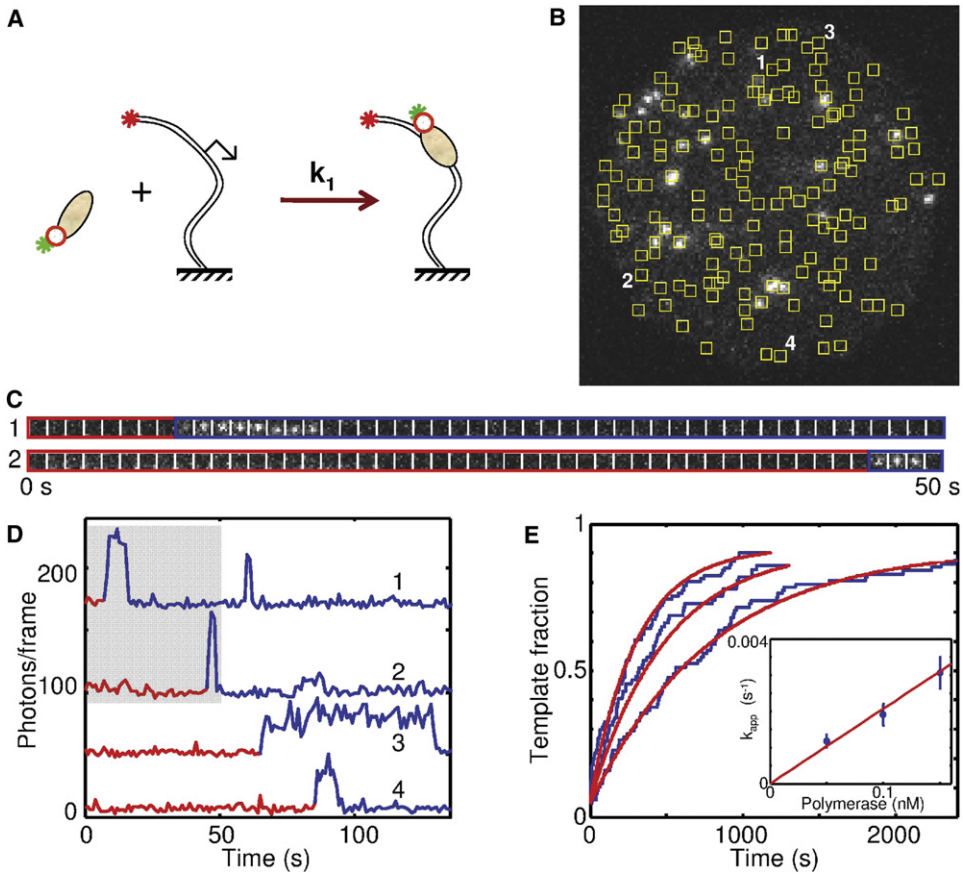

Figure 2. Formation of Closed Complexes

(A) Experimental design. Cy3-σ^{54}RNAP (0.15 nM) is added at time t = 0 to surface-tethered Cy5-template molecules (symbols same as Figure 1A).

(B) Cy3-RNAP spots (ex 532 nm; em < 635 nm) at t = 31 s; image 18.1 × 18.1 μm; integration time 3 s. Positions of Cy5-template spots (yellow squares) were observed prior to RNAP addition.

(C) Time series images of Cy3 fluorescence from template molecules 1 and 2 in (B). Integration time 1 s; images 1.1 × 1.1 μm. Time interval up to the first binding of Cy3-σ^{54}RNAP is highlighted (red).

(D) Cy3 fluorescence intensity records from template molecules 1 through 4 in (B) (traces offset for clarity). Shading marks data shown in (C).

(E) Fraction of template molecules that bound RNAP at least once prior to the indicated time in experiments at 0.05, 0.10, and 0.15 nM RNAP (blue; n = 73, 62, and 85) and exponential fits (red) yielding the fraction of binding-competent template molecules (0.92) and k_{app}, the apparent first-order association rate constants. Inset: Concentration dependence of *k*app (blue); values were corrected as described (Extended Experimental Procedures) and fit (red) yielding second-order binding rate constant $k_1 = (2.1 \pm 0.2) \times 10^7\ M^{-1}\ s^{-1}$.

Error bars reflect standard errors. See also Figure S2.

We considered kinetic schemes with two closed complexes in alternative arrangements to that in scheme 1, but these are either contradicted or rendered less plausible by additional data (Extended Experimental Procedures and Figure S4).

The Rate-Limiting Process in Initiation

Activators of σ^{54} promoters function by accelerating the isomerization from closed to open complexes; it was suggested that this step is rate limiting even at maximal activation (Sasse-Dwight and Gralla, 1988). To definitively establish that the isomerization is rate limiting, we measured the rate of the overall initiation process by adding to tethered DNA a near-saturating concentration of NtrC together with the probe oligo and the full set of reactants needed to initiate transcription (Figure 4A). Cy5 spots reporting the synthesis of new transcripts appeared over hundreds of seconds (Figure 4B), far slower than the time required for hybridization alone ($\tau \sim 9$ s for 10 nM Cy5 probe; see Extended Experimental Procedures). The measured initiation rate (Figure 4C) is > 100-fold slower than formation of either closed complex (scheme 1 and Extended Experimental Procedures). Thus, the rate-limiting step of initiation must follow closed complex formation. Controls show that the limiting rate measured in our experiments is not appreciably affected by labeling of DNA or RNAP, surface tethering of the DNA, or oligo hybridization (Extended Experimental Procedures and Figure S5).

Differentiating Nonproductive and Productive Promoter Binding Events

The foregoing analysis suggests that, even at maximal activation, binding of a σ^{54}RNAP molecule to promoter often fails

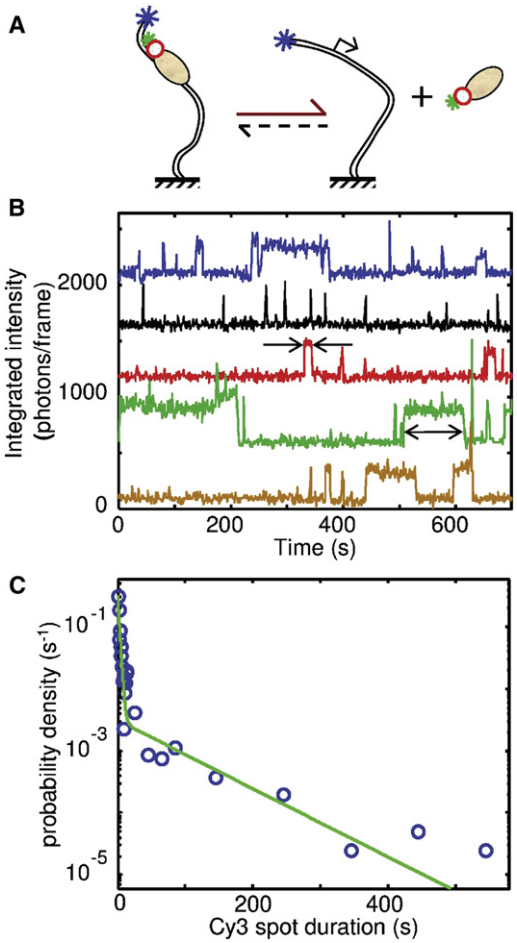

Figure 3. Breakdown of Closed Promoter Complexes

(A) Experimental design. Cy3-σ^{54}RNAP bound and dissociated at equilibrium to surface-tethered AF488-template molecules.

(B) Cy3 intensity records from five individual template locations (offset for clarity). Lifetimes of individual polymerase-template complexes were measured as the durations of intervals of high fluorescence (arrows).

(C) Lifetime distribution of promoter-specific complexes. Binned lifetimes are plotted as corrected probability densities (circles; see Extended Experimental Procedures) overlaid with a biexponential distribution (line) with time constants $\tau_S = 2.3 \pm 0.5$ s, $\tau_L = 79 \pm 13$ s and amplitudes $a_S = 0.76 \pm 0.03$, $a_L = (1 - a_S)$. See also Figure S3.

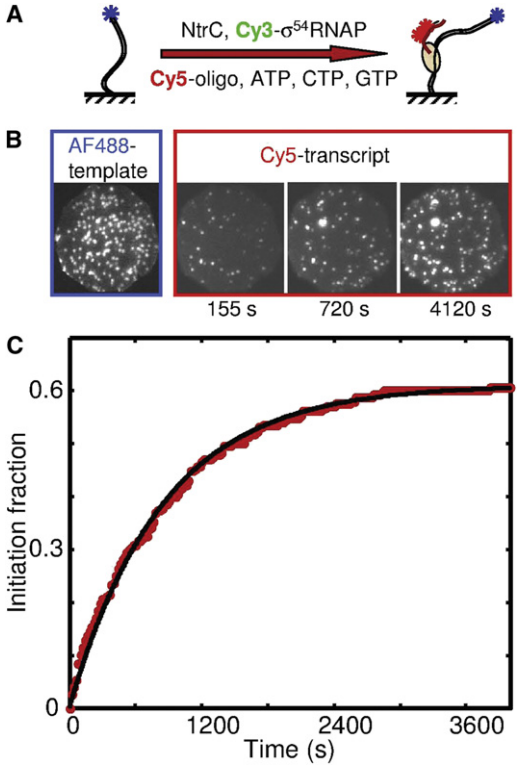

Figure 4. Overall Initiation Rate

(A) Experimental design; RNAP was at 8 nM.

(B) Image of template molecules taken before RNAP addition (blue) and selected images (red) from a recording of probe hybridization at times after RNAP addition (frame duration 1 s).

(C) Template spot fraction that had a colocalized probe spot at or before the time shown (red). Exponential fit (black) yields initiation rate $(1.2 \pm 0.1) \times 10^{-3}$ s^{-1} and active fraction 0.61 (n = *145*).

See also Figure S5.

to produce transcript, with RNAP instead dissociating before the slow open complex formation step has a chance to occur. In this circumstance, it is difficult in bulk experiments to define the characteristics specific to the small minority of binding events that are productive. In contrast, single-molecule experiments allow direct characterization of the productive subpopulation. We used three-color CoSMoS to simultaneously observe RNAP binding to and transcript production from the same template molecule. During the reaction, RNAP spots repeatedly appeared and then disappeared (Figure 5A, green trace) at locations of DNA molecules. For most of these RNAP binding events, we did not detect associated transcript production. However, on most DNAs, we eventually saw a particular RNAP binding (Figure 5A, green square) and subsequent Cy3-σ^{54} departure that was followed within seconds by probe hybridization (red square), suggesting that we observed binding of the particular polymerase molecule that synthesized the transcript. Unlike RNAP spots, probe spots were long lived, often persisting for hundreds of seconds (Figure 5A, red trace, and Movie S1). This is consistent with the production of transcript stably associated with the elongation complex.

To show that we correctly identify the productive RNAP binding events, we examined the time interval Δt_{hyb} separating the appearance of probe hybridization and the most recent departure of a Cy3-σ^{54} spot on the same template (Figure 5A). The Δt_{hyb} distribution is peaked (Figure 5B, blue), whereas a control analysis in which randomly generated values were substituted in place of the observed times of probe hybridization yielded a flat distribution (red). Thus, the characteristically short time between σ^{54} departure and transcript detection does not arise from chance alone. These data imply that we reliably detect the RNAP binding event that leads to production of each transcript.

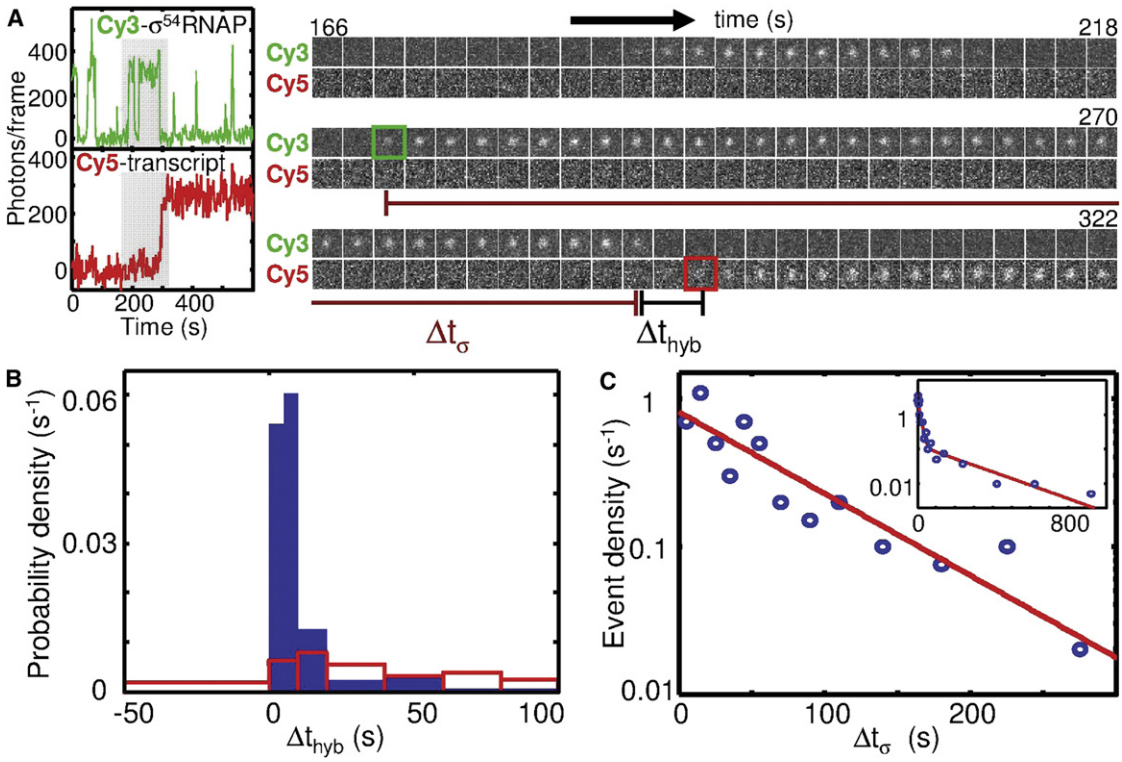

Figure 5. Characterization of RNAP Binding Events that Lead to Transcript Production

Reaction was the same as in Figure 4A but with 0.8 nM RNAP and 20 nM probe.

(A) Fluorescence from RNAP at the location of a single DNA molecule (em < 635 nm) and transcript probe (em > 635 nm). (Left) RNAP and transcript probe emission recording. (Right) Time series of images (1 × 1 μm, 2 s frame duration with 2 frame running average) from the shaded interval in the recordings (series is split into three rows with paired Cy3 [top] and Cy5 [bottom] images at each time). For the initiation event (green and red squares; see text), the apparent duration of the Cy3-σ^{54} presence on the template (Δt_σ) and the time interval separating Cy3-σ^{54} departure from a transcript probe hybridization (Δt_{hyb}) are marked.

(B) (Blue) Normalized histogram showing 53 of 63 measurements of Δt_{hyb} (the remaining ten measurements are outside of the plotted range). By convention, we take Δt_{hyb} to be positive when the Cy5 hybridization signal appears on a template *after* Cy3-σ^{54} has departed. (Red) A control randomized analysis of the same data (see text).

(C) Distribution Δt_σ (circles) for all 63 binding events that most closely preceded transcript detection. Exponential fit (line) yields time constant 78 ± 10 s. (Inset) Distribution of Δt_σ from the randomized sampling control used in (B) (red).

See also Figure S6 and Movie S1.

Open Complexes Form from a Long-Lived Closed Complex Intermediate

In productive RNAP binding events, σ^{54} departure was almost always followed by hybridization of the probe to the transcript within a median Δt_{hyb} ~8 s (Figure 5B), a delay similar to the time required for probe hybridization alone (4.5 s at 20 nM probe). Thus, commencement of transcript synthesis is simultaneous with or closely followed by σ^{54} release.

Because σ^{54} release in the initiating subpopulation reports the start of transcript synthesis, we can measure the time required for productive initiation as the interval between σ^{54}RNAP binding and σ^{54} departure, Δt_σ (Figure 5A). The Δt_σ distribution is exponential (Figure 5C). In contrast, a control analysis on a random sample of polymerase binding events (nearly all of which are nonproductive) yields a biexponential distribution (Figure 5C, inset) similar to the full closed complex lifetime distribution (Figure 3B). Thus, productive events are a subpopulation with distinct kinetic properties. That the average Δt_σ (78 ± 10 s; Figure 5C) is exponential and identical within experimental uncertainty to the long-lived closed complex time constant (73 ± 11 s under these conditions; Figure S6) strongly suggests that the long-lived closed complex RP_2 is a required precursor to formation of open complex and subsequent initiation.

Open Complexes Are Committed to Transcript Elongation

We next examined the fates of open complexes. Addition to open complexes of NTPs at ≥ 500 μM resulted in departure of σ^{54} subunit and transcript production (Figure 6A, right, Figure 6B, and Movie S2). Most σ^{54} spots departed within 10 s (63 of 77; Figure 6C). Most transcript probe spots appeared within ~20 s of σ^{54} departure (Figure S7), as was observed for the overall initiation reaction (Figure 5B). Inclusion of NtrC in the reaction does not substantially alter the outcome, as expected because NtrC was not required to maintain the open state (Figure 1). In one example (Figure 6C), 94% (86 of 91) of open complexes were active (i.e., lost σ^{54}), and probe hybridization was seen on nearly all of these (91%; 78 of 86) by the

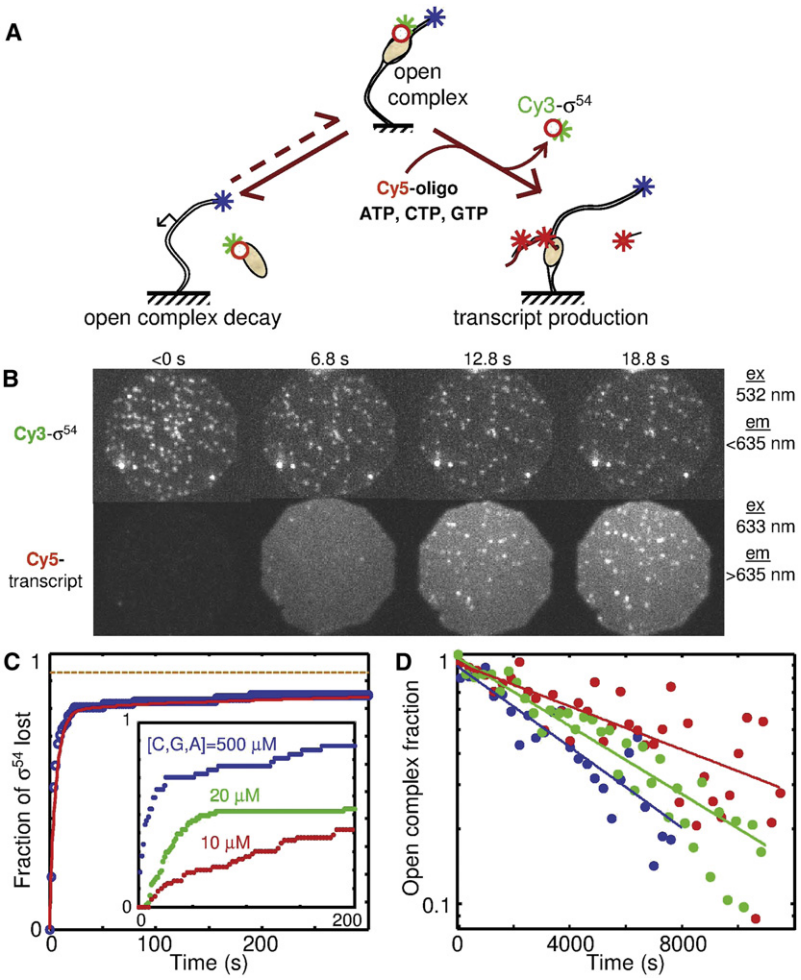

Figure 6. Fates of Open Promoter Complexes

(A) Experimental designs. Open promoter complexes (as in Figure 1D) were incubated in the absence of free RNAP for > 15 min to dissociate any residual closed complexes and then were subjected to conditions that allowed either spontaneous dissociation (left) or transcript production (right).

(B) Images from a recording of transcript production from open complexes upon addition of 1 mM ATP, 0.5 mM CTP, 0.5 mM GTP, and 5 nM probe.

(C) Fraction of open complexes that lost σ^{54} prior to the indicated time and that also synthesized transcript (n = 91). Transcript production reaction in 4 mM ATP, 0.5 mM CTP, 0.5 mM GTP, 5 nM Cy5 probe plus NtrC. Dashed line indicates fraction of active complexes as judged by σ^{54} departure. Biexponential fit (line) yields rate constants 0.17 and 4.3 × 10^{-3} s^{-1} and amplitudes 0.92 and 0.08, respectively. (Inset) Similar experiments performed without NtrC and at reduced NTP concentrations (n = 47 to 81).

(D) Dissociation of open complexes in buffer (blue) plus 4 mM ATP (green) and plus ATP and NtrC (red). (Circles) Photobleaching-corrected fraction of complexes containing Cy3-σ^{54}; (lines) exponential fits yielding rates of 1.9 ± 0.2 × 10^{-4}, 1.57 ± 0.08 × 10^{-4}, and 1.0 ± 0.1 × 10^{-4} s^{-1}, respectively. Each experiment sampled nine fields of view with initial averages of 42, 44, and 31 open complexes in each field, respectively.

See also Figure S7, Table S1, and Movie S1.

reaction endpoint (566 s). Thus, open complexes are efficiently converted into productive elongation complexes; there is no evidence for significant nonproductive dissociation of RNAP during promoter escape.

The σ^{54} open complex has been proposed to be extraordinarily kinetically stable (Tintut et al., 1995; Wedel and Kustu, 1995). We tested this by incubating open complexes with/without ATP and/or NtrC and measured the dissociation rate (Figure 6D). Dissociation was slower with ATP, probably because templated binding of ATP (A is the first base of the transcript) stabilizes the complex. In the presence of both NtrC and ATP, dissociation was slowed even more. Quantitative analysis (see Extended Experimental Procedures and Table S1) showed that reopening of closed complexes produced by open complex decay is not sufficient to account for this difference, suggesting that NtrC and ATP bind to and stabilize open complexes. In all cases, dissociation rates were roughly 10^{-4} s^{-1}, >1,000-fold slower than conversion of open complexes to elongation complexes in the presence of NTPs. Therefore, once the promoter-bound polymerase forms an active open complex at physiological NTP concentrations, it nearly always produces transcript. This conclusion is consistent with the high yields of transcript observed in both the steady-state (Figure 5) and preformed open complex (Figures 6B and 6C) experiments.

σ^{54} Dissociation from the Transcription Complex Requires RNA Synthesis

Rapid departure of σ^{54} from open complexes was observed only in the presence of NTPs. When the concentration of NTPs was lowered, the time for σ^{54} to depart increased (Figures 6C, inset, and S7). This is consistent with the hypothesis that release of σ^{54} from open complexes requires the synthesis of some minimal length of RNA. Reducing NTP concentrations also increases the fraction of complexes that do not release σ^{54} after even lengthy incubation, consistent with the observation that these conditions increase the likelihood of irreversible transcriptional arrest (Erie et al., 1993).

DISCUSSION

A Comprehensive, Quantitative Kinetic Scheme for σ^{54}–Dependent Transcription Initiation

In contrast with the extensive literature on σ^{70} promoters, the kinetic mechanism of initiation at σ^{54} promoters has received comparatively little study. The multiwavelength single-molecule fluorescence experiments reported here comprehensively define a minimal mechanism of initiation at the σ^{54}-dependent *glnAp2* (Figure 7). Features of the σ^{54} initiation pathway revealed in our work include: (1) two closed complex intermediates that likely form in sequence along the reaction path for initiation; (2) both closed complexes are kinetically unstable; (3) NtrC and ATP act on a long-lived closed complex to convert it into an

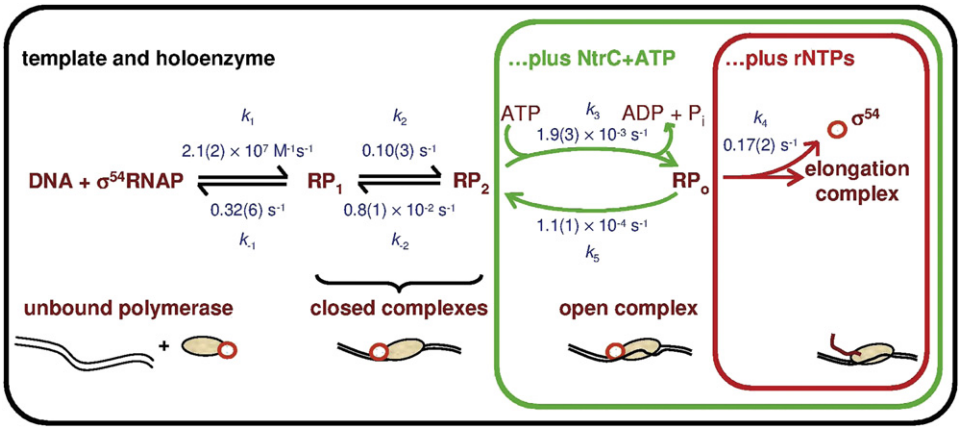

Figure 7. Mechanism of σ^{54}RNAP Initiation

Nested boxes (black, green, and red) specify the combination of reactants needed to produce the different reactions and states. Numbers in parentheses are the standard error of the final digit of the corresponding rate constant. The isomerization step (green) is shown as two separated arrows to denote that the forward reaction, which requires ATP, is not the reverse of the backward reaction, which does not require ADP + P_i.

See also Figure S4 and Table S2.

open promoter complex, and this step remains rate limiting even at maximal activation; (4) even when the RP_2 state is attained, open complex formation is rare; more often, RP_2 nonproductively dissociates without ever reaching the open complex state; overall, RNAP binds to the promoter, on average, 30 times before an open complex is successfully formed; (5) when an open complex is formed, the RNAP is committed to initiation and promptly (in < 10 s) begins transcript synthesis if NTPs are present; (6) σ^{54} is quickly ejected from the complex at the beginning of transcript synthesis. These observations are significant because they provide a mechanistic basis for understanding the regulation of σ^{54}-dependent transcription, as described below.

σ^{54}RNAP Closed Promoter Complexes

Our studies suggest that σ^{54}RNAP forms two different kinds of closed complex, RP_1 and RP_2, and that these most likely occur in sequence along the pathway to open complex formation and transcript initiation, as shown in Figure 7. The existence of two σ^{54} closed complexes was previously unknown, although multiple closed complexes were previously detected for holoenzyme containing the structurally unrelated σ^{70}. Based on the proposed mechanism, RP_2 is the major closed species present in the absence of activator; only $k_{-2} / (k_2 + k_{-2})$ = 7% of the closed complexes exist in the short-lived RP_1 state at equilibrium. Thus, demonstrations that DNA in σ^{54}RNAP closed complexes is not significantly bent (Cannon et al., 1993) implies that DNA in the RP_2 complex is not stably wrapped around RNAP, as it is in some early σ^{70}RNAP closed complex intermediates (Davis et al., 2007; Saecker et al., 2011; Sclavi et al., 2005). On the other hand, footprinting of σ^{54}RNAP closed complexes revealed an "early melted" DNA structure in which the −11 base pair was disrupted (Cannon et al., 2000; Morris et al., 1994). Our analysis suggests that it is RP_2 that contains this nonduplex DNA structure, and our working model is that melting at −11 is the principal structural change corresponding to conversion of RP_1 into the more stable RP_2.

Activation and Isomerization

The proposed initiation mechanism (Figure 7) emphasizes the central importance of the closed-to-open isomerization in the regulation of σ^{54} promoters. RP_2 to RP_o is by far the slowest forward step in the pathway even at conditions of near maximal activation. This is likely also true in live cells, as footprinting showed that *glnAp2* is occupied by closed complexes even when cells are grown in excess nitrogen; open complexes are not detected unless transcript elongation is inhibited (Sasse-Dwight and Gralla, 1988).

Isomerization is highly unfavorable in the absence of activator. In experiments without NtrC (e.g., Figure S1), if initiation occurs at all, its rate must be < 6.0×10^{-6} s^{-1}. Comparison of this value with k_3 shows that activator accelerates initiation by > 300-fold. In addition, the open complex breakdown (k_5 in Figure 7) is modestly slowed (by 0.7; see Figure 6D and Extended Experimental Procedures) by NtrC and ATP. These opposite effects that NtrC+ATP has on open complex formation and breakdown show that NtrC plays an active role in open complex formation: the data cannot be explained if the activator merely stabilizes a transition state or intermediate in the reaction. The data also show that conversion of RP_2 to RP_o is energetically unfavorable in the absence of NtrC, consistent with prior suggestions (Wedel and Kustu, 1995). Specifically, the ratio of the forward and reverse rate constants (< 6.0×10^{-6} s^{-1} / 1.9×10^{-4} s^{-1}; Table S1) constrains the equilibrium constant to be < 0.03, corresponding to ΔG^o > +8.4 kJ/mol. Thus, isomerization must be coupled to a source of energy, presumably from NtrC-σ^{54}RNAP binding energy and/or NtrC ATP hydrolysis.

The σ^{54}-mediated closed-to-open complex isomerization (k_3 in Figure 7) is known to include multiple substeps. First, enhancer-bound activator loops the DNA so that activator can contact σ^{54} and the promoter (Huo et al., 2006). Then, one or more steps in the cycle of activator ATP hydrolysis take place (Burrows et al., 2009; Chen et al., 2007), coupled to reconfiguration of the σ^{54} subunit (Bose et al., 2008; Burrows et al., 2008;

Cannon et al., 2000; Wedel and Kustu, 1995). Finally, additional structural rearrangements position the melted template strand inside the active site cleft. Our experiments demonstrate that, at some point in isomerization, the transcription complex becomes committed to initiation (k_5 versus k_4, Figure 7) and that the key commitment event must either be, or occur after, the rate-limiting substep for open complex formation. Assuming that DNA looping is readily reversible, σ^{54} reconfiguration or DNA melting/template strand binding are the strongest candidates for the step that commits the complex to transcript synthesis.

σ^{54} Is Released upon Promoter Clearance

In principle, σ can have one of three fates when core RNAP escapes from the promoter during initiation. σ may (1) remain bound at the promoter, (2) be retained in the departing elongation complex, or (3) be released into solution. At σ^{70} promoters, a mixture of (2) and (3) is observed (Bar-Nahum and Nudler, 2001; Deighan et al., 2011; Kapanidis et al., 2005). For σ^{54} promoters, the extents of (2) and (3) have not been measured, and there is indirect evidence both for and against (1) at *glnAp2* (Bondarenko et al., 2002; Tintut et al., 1995). We observed almost exclusively (3), with > 90%–95% of complexes releasing σ^{54} before transcript is detected. Efficient release of σ^{54} may be significant to regulation because σ factors can compete with proteins (e.g., NusG) that bind to elongation complexes and regulate their activity (Mooney et al., 2005).

Implications for σ^{54} Promoter Regulation

Although σ^{54} promoters drive genes for a wide variety of biological functions, they share the common feature that they are tightly regulated (Reitzer and Schneider, 2001; Wigneshweraraj et al., 2008). A key benefit of knowing the pathway and kinetics for initiation (Figure 7) is that this information is essential to identify reaction steps that are potential regulatory targets and to understand how different regulatory inputs at different steps can be integrated.

Changing the relative amounts of RNAPs containing alternative σ factors regulates subsets of promoters in response to metabolic conditions (Grigorova et al., 2006; Ishihama, 2000; Lee et al., 2010; Mooney et al., 2005) and, in particular, is thought to globally regulate transcription from σ^{54} promoters (Bernardo et al., 2006; Szalewska-Palasz et al., 2007). σ^{54} promoters are mostly occupied by RNAP closed complexes both in vivo and in vitro (Ninfa et al., 1987; Reitzer et al., 1987; Sasse-Dwight and Gralla, 1988). However, we showed that *glnAp2* closed complexes are dynamic, with RNAP releasing from and rebinding to the promoter frequently, which suggests that, even when a promoter is not activated, bound RNAP exchanges with the cellular pool, thus allowing promoter occupancy to change in response to changes in expression of alternate σ factors.

Regulation of bacterial transcription initiation is effected primarily by modulation of one or more of the principal stages of initiation: promoter binding, isomerization, and promoter escape. At σ^{70} promoters, there are examples of regulators that act at each of these stages (Browning and Busby, 2004). In contrast, we show that, at the σ^{54} promoter studied here, initiation kinetics have a striking feature: once open complexes form at physiological NTP concentrations, they are committed to promoter escape and transcript synthesis. Assuming that the same is true in vivo, this kinetic profile significantly limits the possible mechanisms of regulation: activators cannot easily act at the promoter escape step because open complexes are already committed to elongation. Specifically, repression at this step would be limited to negative regulators strong enough to slow promoter escape by > ~1,000-fold so that escape starts to limit the overall rate of initiation. This may be a constraint to regulation of σ^{54} promoters in general: enhancer binding proteins appear to act exclusively at the isomerization step, and we know of no evidence for regulation of promoter escape by σ^{54}RNAP.

Even at the high activator concentrations used here, the isomerization step limits the overall rate of initiation (Figure 7). This suggests that factors that alter the probability of contact between enhancer-bound activator and the promoter-bound σ^{54}RNAP (e.g., by bending DNA or altering its flexibility) can repress or further activate transcription from σ^{54} promoters even in the presence of maximal activator concentrations. This feature of the mechanism is consistent with studies that show that DNA supercoiling or DNA bending or stiffening proteins can substantially alter initiation rates at some σ^{54} promoters (Amit et al., 2011; Huo et al., 2006).

Conclusions

We report experiments that follow the initiation reaction from start to finish, define key intermediates, and measure the full set of rates connecting the intermediates. The deduced mechanism provides the essential underpinning for quantitative understanding of promoter regulation, identifying key constraints to and opportunities for regulation. The CoSMoS method should be broadly applicable to studying other transcriptional regulation systems in both prokaryotes and eukaryotes and raises the possibility of further elucidation of regulatory mechanisms by simultaneously monitoring both RNAP dynamics and binding of transcription factors to the same promoter in real time.

EXPERIMENTAL PROCEDURES

DNA and Plasmids

The 853 bp transcription template (Figure 1A) containing the *S. typhimurium glnAp2* promoter region and a strong enhancer was prepared by PCR (see Extended Experimental Procedures) from pJES534. The Cy5-labeled antisense probe (see Extended Experimental Procedures) was complementary to 20 of the 21 nt in the repeat cassette.

Protein Expression and Purification

Core *E. coli* RNAP was obtained from Epicenter (Madison, WI). Expression plasmids pNtrC-2 and pS54-2 were gifts from Karsten Rippe (Rippe et al., 1997). pNtrC-2 encodes *Salmonella typhimurium* $NtrC^{D54E,S160F}$ with the N-terminal His tag and linker HHHHHHSSGLVPRGSH. $NtrC^{D54E,S160F}$ is a constitutively active mutant that does not require phosphorylation in order to activate transcription (Klose et al., 1993). pS54-2 encodes *Escherichia coli* σ^{54} with the same His tag and linker. pS54-4 is identical to pS54-2 except that all endogenous Cys residues were mutated (C198A C307G C346A), and a new Cys was substituted for the underlined Gly in the linker. The proteins were expressed in *E. coli* BL21(DE3)pLysS and purified as described (Rippe et al., 1997) with minor modifications (Extended Experimental Procedures). Cy3-σ^{54} was prepared by reacting the single cysteine σ^{54} with Cy3 maleimide and had activity essentially identical to wild-type σ^{54} (Figure S5A).

Single-Molecule Microscopy

The microscope for performing multiwavelength single-molecule total internal reflection (TIR) fluorescence microscopy using excitation lasers at 488, 532, and 633 nm has been previously described (Friedman et al., 2006) but incorporated new features (Extended Experimental Procedures). Biotinated, dye-labeled DNA molecules were linked with streptavidin to the surface of a fused silica flow cell essentially as described (Friedman et al., 2006). To identify locations of the DNA molecules, one to two images of the fluorescent label were acquired at the beginning and/or end of the experiment. Reactions with RNAP were performed in transcription buffer containing 50 mM Tris-OAc (pH 8.0), 100 mM KOAc, 8 mM MgOAc, 27 mM NH_4OAc, 2 mM dithiothreitol, 3.5% (w/v) polyethylene glycol 8000 (#81268 Sigma-Aldrich; St. Louis, MO), 0.1 mg/ml bovine serum albumin (#126615 EMD Chemicals; La Jolla, CA), and an oxygen scavenging system to minimize photobleaching (Friedman et al., 2006). Unless otherwise specified, reactants were 0.8 nM σ^{54}RNAP, 14 nM dimer $NtrC^{D54E,\ S160F}$, 4 mM ATP, 0.5 mM CTP, 0.5 mM GTP, and 10 nM Cy5-oligo.

Analysis of CoSMoS Data

Analysis of single-molecule colocalization data was performed with custom software implemented in Matlab. In cases in which the emission was separated into long- and short-wavelength images, a transformation matrix that superimposes the two images was first calculated using a calibration sample containing single molecules that were visible in both images. In experiments in which individual molecules were followed in time, images were separately corrected for sample movement upon introduction of reagents and for stage drift by Gaussian fitting of selected fluorescent spots. To score association and release of labeled molecules (σ^{54} or transcript probe oligonucleotide) from a surface-tethered DNA molecule, we integrated the fluorescence emission of the molecules over a 0.25 μm^2 area centered at DNA locations. A small baseline drift in these emission time courses was removed by subtracting segments of the record to which a low-pass filter had been applied. In the resulting records, increases to an emission intensity > 3.6 times the standard deviation of the baseline noise were scored as a binding event. Each event was subsequently inspected visually, and those that did not correspond to a well-defined spot of fluorescence centered at the DNA position were discarded. Following a binding event, the first decrease of the emission to < 1.0 times the standard deviation of the baseline noise was scored as dissociation. For kinetic analysis, measured time intervals were fit using maximum likelihood methods, and fit parameter error distributions were estimated by bootstrapping. For cases in which rate constants were a function of more than one fit parameter, the rate constants were calculated from the fit parameters by iterative optimization using the Q-matrix method (Colquhoun, 1995) or equivalent (e.g., Figure S5). Error estimates for the rate constants were calculated by error propagation from the fit parameter error distributions using bootstrapping.

SUPPLEMENTAL INFORMATION

Supplemental Information includes Extended Experimental Procedures, seven figures, two tables, and two movies and can be found with this article online at doi:10.1016/j.cell.2012.01.018.

ACKNOWLEDGMENTS

We thank K. Rippe for plasmids and A. Hochschild, A. Hoskins, R. Landick, M. Marr, J. Mumm, and M. Osborne for helpful discussions. This work was supported by grants K25 GM00714 (to L.J.F.), R01 GM43369, and R01 GM81648 (to J.G.) from the NIGMS.

Received: June 7, 2011
Revised: September 26, 2011
Accepted: January 5, 2012
Published: February 16, 2012

REFERENCES

Amit, R., Garcia, H.G., Phillips, R., and Fraser, S.E. (2011). Building enhancers from the ground up: a synthetic biology approach. Cell *146*, 105–118.

Bar-Nahum, G., and Nudler, E. (2001). Isolation and characterization of σ^{70}-retaining transcription elongation complexes from Escherichia coli. Cell *106*, 443–451.

Bernardo, L.M., Johansson, L.U., Solera, D., Skärfstad, E., and Shingler, V. (2006). The guanosine tetraphosphate (ppGpp) alarmone, DksA and promoter affinity for RNA polymerase in regulation of σ^{54}-dependent transcription. Mol. Microbiol. *60*, 749–764.

Bondarenko, V., Liu, Y., Ninfa, A., and Studitsky, V.M. (2002). Action of prokaryotic enhancer over a distance does not require continued presence of promoter-bound σ^{54} subunit. Nucleic Acids Res. *30*, 636–642.

Bose, D., Pape, T., Burrows, P.C., Rappas, M., Wigneshweraraj, S.R., Buck, M., and Zhang, X. (2008). Organization of an activator-bound RNA polymerase holoenzyme. Mol. Cell *32*, 337–346.

Browning, D.F., and Busby, S.J. (2004). The regulation of bacterial transcription initiation. Nat. Rev. Microbiol. *2*, 57–65.

Buck, M., Gallegos, M.T., Studholme, D.J., Guo, Y., and Gralla, J.D. (2000). The bacterial enhancer-dependent σ^{54} (σ^{N}) transcription factor. J. Bacteriol. *182*, 4129–4136.

Burrows, P.C., Joly, N., Cannon, W.V., Cámara, B.P., Rappas, M., Zhang, X., Dawes, K., Nixon, B.T., Wigneshweraraj, S.R., and Buck, M. (2009). Coupling σ factor conformation to RNA polymerase reorganisation for DNA melting. J. Mol. Biol. *387*, 306–319.

Burrows, P.C., Wigneshweraraj, S.R., and Buck, M. (2008). Protein-DNA interactions that govern AAA+ activator-dependent bacterial transcription initiation. J. Mol. Biol. *375*, 43–58.

Cannon, W., Claverie-Martin, F., Austin, S., and Buck, M. (1993). Core RNA polymerase assists binding of the transcription factor σ^{54} to promoter DNA. Mol. Microbiol. *8*, 287–298.

Cannon, W.V., Gallegos, M.T., and Buck, M. (2000). Isomerization of a binary sigma-promoter DNA complex by transcription activators. Nat. Struct. Biol. *7*, 594–601.

Cases, I., de Lorenzo, V., and Ouzounis, C.A. (2003). Transcription regulation and environmental adaptation in bacteria. Trends Microbiol. *11*, 248–253.

Chen, B., Doucleff, M., Wemmer, D.E., De Carlo, S., Huang, H.H., Nogales, E., Hoover, T.R., Kondrashkina, E., Guo, L., and Nixon, B.T. (2007). ATP ground- and transition states of bacterial enhancer binding AAA+ ATPases support complex formation with their target protein, σ54. Structure *15*, 429–440.

Colquhoun, D.H.A.G. (1995). A Q Matrix Cookbook. In Single Channel Recording, Second Edition, B. Sakmann and E. Neher, eds. (New York: Plenum Publishing Corporation), pp. 589–633.

Crawford, D.J., Hoskins, A.A., Friedman, L.J., Gelles, J., and Moore, M.J. (2008). Visualizing the splicing of single pre-mRNA molecules in whole cell extract. RNA *14*, 170–179.

Darst, S.A. (2004). New inhibitors targeting bacterial RNA polymerase. Trends Biochem. Sci. *29*, 159–160.

Davis, C.A., Bingman, C.A., Landick, R., Record, M.T., Jr., and Saecker, R.M. (2007). Real-time footprinting of DNA in the first kinetically significant intermediate in open complex formation by Escherichia coli RNA polymerase. Proc. Natl. Acad. Sci. USA *104*, 7833–7838.

Deighan, P., Pukhrambam, C., Nickels, B.E., and Hochschild, A. (2011). Initial transcribed region sequences influence the composition and functional properties of the bacterial elongation complex. Genes Dev. *25*, 77–88.

Erie, D.A., Hajiseyedjavadi, O., Young, M.C., and von Hippel, P.H. (1993). Multiple RNA polymerase conformations and GreA: control of the fidelity of transcription. Science *262*, 867–873.

Friedman, L.J., Chung, J., and Gelles, J. (2006). Viewing dynamic assembly of molecular complexes by multi-wavelength single-molecule fluorescence. Biophys. J. *91*, 1023–1031.

Grigorova, I.L., Phleger, N.J., Mutalik, V.K., and Gross, C.A. (2006). Insights into transcriptional regulation and σ competition from an equilibrium model of RNA polymerase binding to DNA. Proc. Natl. Acad. Sci. USA *103*, 5332–5337.

Halford, S.E. (2009). An end to 40 years of mistakes in DNA-protein association kinetics? Biochem. Soc. Trans. *37*, 343–348.

Haugen, S.P., Berkmen, M.B., Ross, W., Gaal, T., Ward, C., and Gourse, R.L. (2006). rRNA promoter regulation by nonoptimal binding of σ region 1.2: an additional recognition element for RNA polymerase. Cell *125*, 1069–1082.

Ho, M.X., Hudson, B.P., Das, K., Arnold, E., and Ebright, R.H. (2009). Structures of RNA polymerase-antibiotic complexes. Curr. Opin. Struct. Biol. *19*, 715–723.

Hoskins, A.A., Friedman, L.J., Gallagher, S.S., Crawford, D.J., Anderson, E.G., Wombacher, R., Ramirez, N., Cornish, V.W., Gelles, J., and Moore, M.J. (2011). Ordered and dynamic assembly of single spliceosomes. Science *331*, 1289–1295.

Huo, Y.X., Tian, Z.X., Rappas, M., Wen, J., Chen, Y.C., You, C.H., Zhang, X., Buck, M., Wang, Y.P., and Kolb, A. (2006). Protein-induced DNA bending clarifies the architectural organization of the σ54-dependent *glnA*p2 promoter. Mol. Microbiol. *59*, 168–180.

Ishihama, A. (2000). Functional modulation of Escherichia coli RNA polymerase. Annu. Rev. Microbiol. *54*, 499–518.

Joly, N., Zhang, N., Buck, M., and Zhang, X. (2012). Coupling AAA protein function to regulated gene expression. Biochim. Biophys. Acta. *1823*, 108–116.

Kapanidis, A.N., Margeat, E., Laurence, T.A., Doose, S., Ho, S.O., Mukhopadhyay, J., Kortkhonjia, E., Mekler, V., Ebright, R.H., and Weiss, S. (2005). Retention of transcription initiation factor σ^{70} in transcription elongation: single-molecule analysis. Mol. Cell *20*, 347–356.

Klose, K.E., Weiss, D.S., and Kustu, S. (1993). Glutamate at the site of phosphorylation of nitrogen-regulatory protein NTRC mimics aspartyl-phosphate and activates the protein. J. Mol. Biol. *232*, 67–78.

Kontur, W.S., Saecker, R.M., Capp, M.W., and Record, M.T., Jr. (2008). Late steps in the formation of *E. coli* RNA polymerase-λP_R promoter open complexes: characterization of conformational changes by rapid [perturbant] upshift experiments. J. Mol. Biol. *376*, 1034–1047.

Lee, C.R., Cho, S.H., Kim, H.J., Kim, M., Peterkofsky, A., and Seok, Y.J. (2010). Potassium mediates Escherichia coli enzyme IIA(Ntr) -dependent regulation of sigma factor selectivity. Mol. Microbiol. *78*, 1468–1483.

Lin, Y.C., Choi, W.S., and Gralla, J.D. (2005). TFIIH XPB mutants suggest a unified bacterial-like mechanism for promoter opening but not escape. Nat. Struct. Mol. Biol. *12*, 603–607.

Magasanik, B. (1996). Regulation of Nitrogen Utilization. In Escherichia Coli and Salmonella Cellular and Molecular Biology, F.C. Neidhardt, ed. (Washington, DC: ASM Press), pp. 1344.

Merrick, M.J. (1993). In a class of its own—the RNA polymerase sigma factor σ^{54} (σ^{N}). Mol. Microbiol. *10*, 903–909.

Mooney, R.A., Darst, S.A., and Landick, R. (2005). Sigma and RNA polymerase: an on-again, off-again relationship? Mol. Cell *20*, 335–345.

Morris, L., Cannon, W., Claverie-Martin, F., Austin, S., and Buck, M. (1994). DNA distortion and nucleation of local DNA unwinding within sigma-54 (σ^{N}) holoenzyme closed promoter complexes. J. Biol. Chem. *269*, 11563–11571.

Murakami, K.S., and Darst, S.A. (2003). Bacterial RNA polymerases: the wholo story. Curr. Opin. Struct. Biol. *13*, 31–39.

Ninfa, A.J., Reitzer, L.J., and Magasanik, B. (1987). Initiation of transcription at the bacterial glnAp2 promoter by purified E. coli components is facilitated by enhancers. Cell *50*, 1039–1046.

Popham, D.L., Szeto, D., Keener, J., and Kustu, S. (1989). Function of a bacterial activator protein that binds to transcriptional enhancers. Science *243*, 629–635.

Record, M., Jr., Reznikoff, W., Craig, M., McQuade, K., and Schlax, P. (1996). Escherichia coli and RNA polymerase, promoters, and the kinetics of the steps of transcription initiation. In Escherichia coli and Salmonella: Cellular and Molecular Biology, 2nd Edition, F. Neidhardt, R. Curtiss, III, J. Ingraham, E. Lin, K. Low, B. Magasanik, W. Reznikoff, M. Riley, M. Schaechter, and H. Umbarger, eds. (Washington, DC: ASM Press), pp. 792–821.

Reitzer, L., and Schneider, B.L. (2001). Metabolic context and possible physiological themes of σ^{54}-dependent genes in Escherichia coli. Microbiol. Mol. Biol. Rev. *65*, 422–444.

Reitzer, L.J., Bueno, R., Cheng, W.D., Abrams, S.A., Rothstein, D.M., Hunt, T.P., Tyler, B., and Magasanik, B. (1987). Mutations that create new promoters suppress the σ^{54} dependence of *glnA* transcription in *Escherichia coli*. J. Bacteriol. *169*, 4279–4284.

Revyakin, A., Ebright, R.H., and Strick, T.R. (2004). Promoter unwinding and promoter clearance by RNA polymerase: detection by single-molecule DNA nanomanipulation. Proc. Natl. Acad. Sci. USA *101*, 4776–4780.

Revyakin, A., Liu, C., Ebright, R.H., and Strick, T.R. (2006). Abortive initiation and productive initiation by RNA polymerase involve DNA scrunching. Science *314*, 1139–1143.

Rippe, K., Guthold, M., von Hippel, P.H., and Bustamante, C. (1997). Transcriptional activation via DNA-looping: visualization of intermediates in the activation pathway of E. coli RNA polymerase · σ^{54} holoenzyme by scanning force microscopy. J. Mol. Biol. *270*, 125–138.

Saecker, R.M., Record, M.T., and Dehaseth, P.L. (2011). Mechanism of bacterial transcription initiation: RNA polymerase-promoter binding, isomerization to initiation-competent open complexes, and initiation of RNA synthesis. J. Mol. Biol. *412*, 754–777.

Sasse-Dwight, S., and Gralla, J.D. (1988). Probing the *Escherichia coli glnALG* upstream activation mechanism in vivo. Proc. Natl. Acad. Sci. USA *85*, 8934–8938.

Sasse-Dwight, S., and Gralla, J.D. (1990). Role of eukaryotic-type functional domains found in the prokaryotic enhancer receptor factor σ^{54}. Cell *62*, 945–954.

Sclavi, B., Zaychikov, E., Rogozina, A., Walther, F., Buckle, M., and Heumann, H. (2005). Real-time characterization of intermediates in the pathway to open complex formation by Escherichia coli RNA polymerase at the T7A1 promoter. Proc. Natl. Acad. Sci. USA *102*, 4706–4711.

Susa, M., Kubori, T., and Shimamoto, N. (2006). A pathway branching in transcription initiation in Escherichia coli. Mol. Microbiol. *59*, 1807–1817.

Szalewska-Palasz, A., Johansson, L.U., Bernardo, L.M., Skärfstad, E., Stec, E., Brännström, K., and Shingler, V. (2007). Properties of RNA polymerase bypass mutants: implications for the role of ppGpp and its co-factor DksA in controlling transcription dependent on sigma54. J. Biol. Chem. *282*, 18046–18056.

Tintut, Y., Wang, J.T., and Gralla, J.D. (1995). A novel bacterial transcription cycle involving sigma 54. Genes Dev. *9*, 2305–2313.

Villain-Guillot, P., Bastide, L., Gualtieri, M., and Leonetti, J.-P. (2007). Progress in targeting bacterial transcription. Drug Discov. Today *12*, 200–208.

Wedel, A., and Kustu, S. (1995). The bacterial enhancer-binding protein NTRC is a molecular machine: ATP hydrolysis is coupled to transcriptional activation. Genes Dev. *9*, 2042–2052.

Wigneshweraraj, S., Bose, D., Burrows, P.C., Joly, N., Schumacher, J., Rappas, M., Pape, T., Zhang, X., Stockley, P., Severinov, K., and Buck, M. (2008). Modus operandi of the bacterial RNA polymerase containing the sigma54 promoter-specificity factor. Mol. Microbiol. *68*, 538–546.